The calculated deflection was 0.1956 mm by the formula, which agreed with the hybrid panel tip deflection at 0.1943 mm. By the formula, the deflection was 34% due to shear, which checked the deflection characteristics of the panel.

Figure 2 shows a system of shear panels and rods that is internally redundant on the four cells. The classical force transfer solution given in Ref. 9 is shown and compared to the hybrid method in the figure. A displacement incompatibility between the large element on the left and the four cells was introduced in the hybrid method.

It should be noted that the load transfer mechanism used by the hybrid method is different from the classical force transfer approach of Ref. 9. The hybrid method has a constant force in each rod, while the force approach assumes a linearly varying force. However, there was fairly good agreement between the two methods in the shear flows shown in Fig. 2. This panel could be extended to include a linear varying force in each rod that would be analogous to Ref. 9.

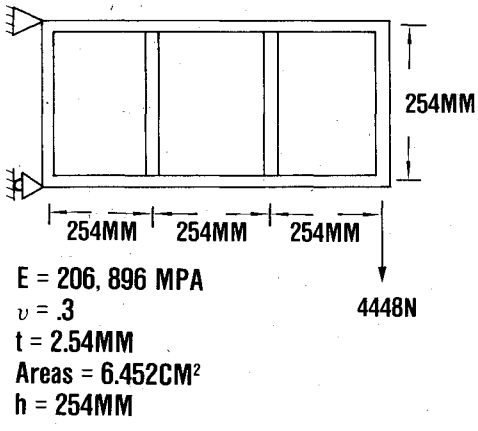


Fig. 1 Shear panel cantilever.

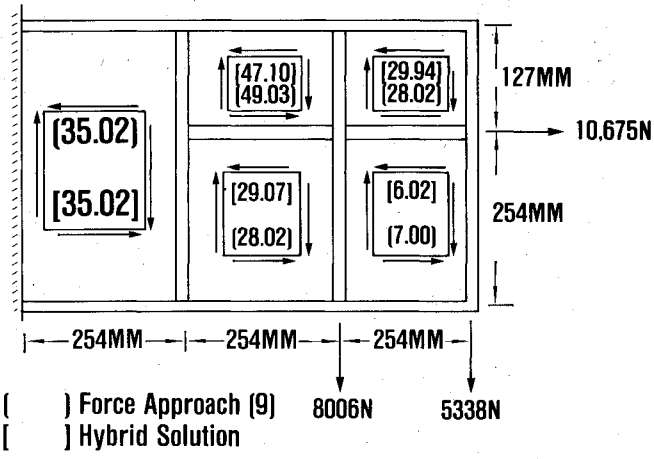


Fig. 2 Shear flows, N/mm².

## Conclusion

The hybrid shear panel takes a constant shear stress along each edge with no normal stress. The panel is compatible only along interelement boundaries and is not compatible within the element. The panel may be distorted into a quadrilateral, although no numerical results could be found in the literature for comparison. Equilibrium is forced at the node points and is not assured everywhere, although the shear stresses along each panel are in equilibrium with the panel.

This panel could be extended to include warpage effects, and extensions could be made to integrate the panel with linear force varying rods to improve the equilibrium characteristics.

## References

[1] MacNeal, R. H., *The NASTRAN Theoretical Manual,* NASA SP-221, 1976.

[2] Garvey, S. J., "The Quadrilateral Shear Panel," *Aircraft Engineering,* May 1951, pp. 134-135.

[3] Robinson, J., "A Six Node Triangular Shear Panel for Equilibrium Models," *RA/ARD,* Rept. No. 25-4-73-14, April 1973.

[4] Kabaila, A. P. and Edwards, R. J., "Hybrid Element Applied to a Shear Wall Analysis," *Journal of Structural Division,* Vol. 105, Dec. 1979.

[5] Cook, R. D. and Al-Abdulla, J. K., "Some Plane Quadrilateral Hybrid Finite Elements," *AIAA Journal,* Vol. 7, Nov. 1979, pp. 2184-2185.

[6] Zienkiewicz, O. C., *The Finite Element Method,* 3rd ed., McGraw-Hill, New York, 1977, pp. 304-325.

[7] Washizu, K., *Variational Methods in Elasticity and Plasticity,* Pergamon Press, New York, 1975, pp. 8-38.

[8] Gallagher, R. H., *Finite Element Analysis Fundamentals,* Prentice-Hall, New Jersey, 1975, pp. 135-210.

[9] Peery, D. J., *Aircraft Structures,* McGraw-Hill, New York, 1950, pp. 181-195.

AIAA 82-4124

# Time-Dependent Adhesive Behavior Effects in a Stepped Lap Joint

M. M. Ratwani,* H. P. Kan,† and D. D. Liu‡
*Northrop Corporation, Hawthorne, Calif.*

## Introduction

INCREASING use of adhesive bonding in aerospace structures requires that analysis methods be available in the areas of service life and strength predictions. Adhesives exhibit viscoelastic (time-dependent) behavior, i.e., the stress-strain relation is a function of time. This behavior will influence stress distribution in adhesively bonded structures. Also, any life prediction technique will be influenced by the viscoelastic behavior of adhesives. Hence, the time-dependent behavior of adhesively bonded structures must be properly understood.

An extensive study of time-dependent behavior of adhesively bonded joints has been carried out by Romanko and Knauss.[1] The method of modeling viscoelastic behavior, based on experimental observations, is also discussed in Ref. 1. For rigid adherends, the influence of time-dependent adhesive behavior on a metal-to-metal bonded joint has been investigated in this reference, and the stress distribution is shown to be time-independent. In reality the adherends are never rigid, and the influence of elastic behavior of adherends should be taken into consideration. The analytical techniques developed by Erdogan and Ratwani[2] for elastic adherends are extended to take into consideration the time-dependent behavior of the adhesives.

## Viscoelastic Model for Adhesive Behavior

The viscoelastic behavior of typical structural adhesives (such as epoxy adhesives FM73 and FM400[1]) can be

Received Jan. 14, 1980; revision received Sept. 14, 1981. 

†Engineering Specialist, Structural Life Assurance Research. Member AIAA.

‡Engineering Specialist, Structural Dynamics Research. Member AIAA.

adequately represented by a standard three-parameter solid,[1] a Maxwell spring, and Voigt-Kelvin model in series as in Fig. 1. Romanko and Knauss[1] show that the time-dependent behavior can be represented by

$$\epsilon = \frac{\sigma}{E_1} + \frac{\sigma}{E_2}\left(1 - e^{-tE_2/\eta_2}\right) \tag{1}$$

where $E_1$ is the initial modulus, $E_2$ the delayed modulus, and $\eta_2$ a constant. The stress-strain relation given in Eq. (1) can be derived easily. The general stress-strain relation for a viscoelastic material is given by[3]

$$\left(1 + a_1 \frac{\partial}{\partial t}\right)\sigma(x,t) = 2k_1\left(1 + b_1 \frac{\partial}{\partial t}\right)\epsilon(x,t) \tag{2}$$

where $a_1$, $b_1$, and $k_1$ are constants.

For $a_1 = 0$ and the stress-strain relation independent of space coordinates, Eq. (2) reduces to

$$\sigma = 2k_1\left(1 + b_1 \frac{\mathrm{d}}{\mathrm{d}t}\right)\epsilon \tag{3}$$

or

$$\frac{\mathrm{d}\epsilon}{\mathrm{d}t} + \frac{1}{b_1}\epsilon = \frac{\sigma}{2k_1 b_1} \tag{4}$$

The solution of Eq. (4) is

$$\epsilon = Ae^{-t/b_1} + (\sigma/2k_1) \tag{5}$$

If the initial strain at time $t=0$ is given as $\sigma/E_1$ and at a time $t=\infty$ is $\sigma/E_1 + \sigma/E_2$, Eq. (5) reduces to

$$\epsilon = \frac{\sigma}{E_1} + \frac{\sigma}{E_2}\left(1 - e^{-t/b_1}\right) \tag{6}$$

This equation is identical to Eq. (1), obtained from experimental results in Ref. 1. The variation of adhesive shear modulus with time for FM73 adhesive is shown in Fig. 1. The curve in Fig. 1 is obtained from the experimental results of Ref. 1 on the assumption that the viscoelastic behavior under shear and extensional stresses is similar. The constants in viscoelastic model, obtained by least-square fit in Ref. 1 for the extensional modulus, have been used to describe the adhesive behavior under shear stresses. Experimental results[4,5] for the shear modulus of adhesive vary from 896 to 379 MPa (130 to 55 ksi), which agree with the values shown in Fig. 1.

## Viscoelastic Analysis of a Bonded Joint

Consider the single-step lap joint shown in the insert in Fig. 2 where an isotropic adherend 1 (constants $E_{1l}$, $\nu_1$) is bonded to an orthotropic adherend 2 (constants $E_{2x}$, $\nu_{2x}$, $E_{2z}$, $\nu_{2z}$, $G_{2xz}$). The joint is subjected to a uniform tensile force $p_0$ at time $t=0$. Thus, the input function is $p_0H(t)$. The problem will be solved under the assumptions that the adherends are under a generalized plane stress ($\sigma_{1y} = \sigma_{2y} = 0$) condition and the adhesive acts as a shear spring.[2] Let $p_1(x,t)$ and $p_2(x,t)$ be the forces in plates 1 and 2, respectively, and $\tau(x,t)$ be the shear stress in the adhesive layer. From equilibrium of adherend 2 and the adhesive layer,

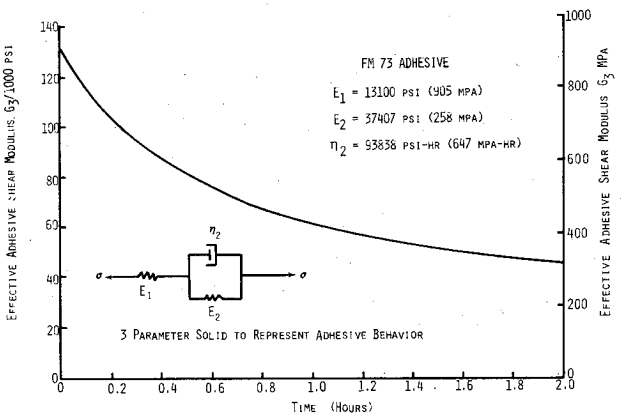


**Fig. 1 Variation of effective shear modulus ($G_3 = \tau/\epsilon$) of FM73 adhesive.**

$$p_2(x,t) = \int_0^x \tau(x,t)\,\mathrm{d}x \tag{7}$$

$$\tau(x,t) = \frac{G_3}{h_3}\left[u_2(x,t) - u_1(x,t)\right] \tag{8}$$

where $G_3$ is the shear modulus of the adhesive. For a plane strain case (in the $z$ direction)

$$\epsilon_{1z}(x,t) = \epsilon_{2z}(x,t) = 0 \tag{9}$$

Under this assumption $\sigma_{1z}(x,t) = \nu_1\sigma_{1x}(x,t)$ and $\sigma_{2z}(x,t) = \nu_{2z}\sigma_{2x}(x,t)$. The force in plate 1 and the stresses in the adherends are given by:

$$p_1(x,t) = p_0H(t) - p_2(x,t)$$

$$\sigma_{1x}(x,t) = \frac{p_1(x,t)}{h_1}, \quad \sigma_{2x}(x,t) = \frac{p_2(x,t)}{h_2} \tag{10}$$

The strains in the adherends are given by the stress-strain relations as

$$\epsilon_{1x}(x,t) = \frac{1-\nu_1^2}{E_{1l}h_1}\left[p_0H(t) - p_2(x,t)\right]$$

$$\epsilon_{2x}(x,t) = \frac{1-\nu_{2x}\nu_{2z}}{E_{2x}h_2}p_2(x,t) \tag{11}$$

and the strain-displacement relations are

$$\epsilon_{1x}(x,t) = \frac{\partial u_1(x,t)}{\partial x}, \quad \epsilon_{2x}(x,t) = \frac{\partial u_2(x,t)}{\partial x} \tag{12}$$

The Laplace transforms of $p_2(x,t)$ and $\tau(x,t)$ are

$$\bar{p}_2(x,s) = \int_0^\infty p_2(x,t)e^{-st}\mathrm{d}t, \quad \bar{\tau}(x,s) = \int_0^\infty \tau(x,t)e^{-st}\mathrm{d}t \tag{13}$$

Similarly, the Laplace transforms of other stress, strain, and displacement quantities can be defined using Eqs. (7), (8), (11), and (12); the problem reduces to the solution of the ordinary differential equation

$$\frac{\mathrm{d}^2\bar{p}_2(x,s)}{\mathrm{d}x^2} - \alpha^2\bar{p}_2(x,s) = \beta p_0 \tag{14}$$

where

$$\alpha^2 = \frac{2k_1(1+b_1s)}{(1+a_1s)h_3}\left[\frac{1-\nu_1^2}{E_{1l}h_1} + \frac{1-\nu_{2x}\nu_{2z}}{E_{2x}h_2}\right]$$

$$\beta = -\frac{2k_1(1+b_1s)}{(1+a_1s)s}\frac{(1-\nu_1^2)}{E_{1l}h_1} \tag{15}$$

The solution to Eq. (14), subjected to the boundary conditions $\bar{p}(0,s) = 0$ and $\bar{p}(\ell,s) = 1/s$, is:

$$\bar{p}_2(x,s) = p_0\left\{(1+c)\frac{\sinh(\alpha x)}{s\cdot\sinh(\alpha\ell)} + c\frac{\sinh[\alpha(\ell-x)]}{s\cdot\sinh(\alpha\ell)} - \frac{c}{s}\right\} \tag{16}$$

where

$$c = -1\Big/\left[1 + \frac{1-\nu_{2x}\nu_{2z}}{1-\nu_1^2}\frac{E_{1l}h_1}{E_{2x}h_2}\right]$$

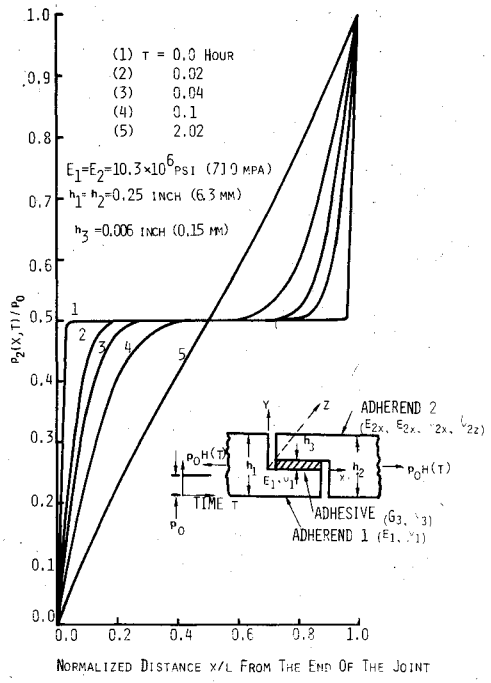


**Fig. 2 Variation of force in adherend 2 with distance from the end of the joint.**

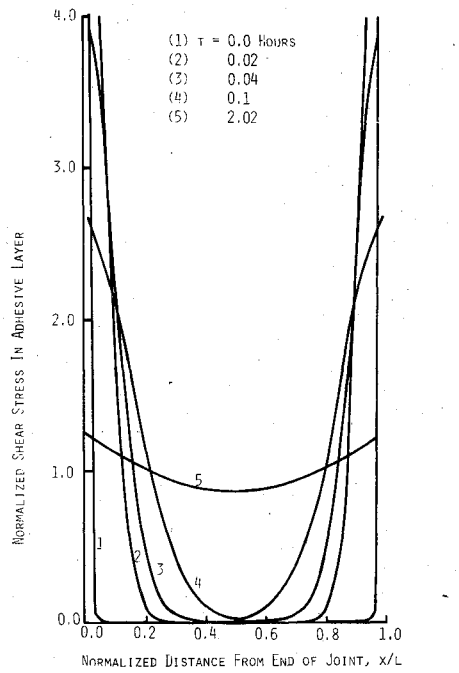


**Fig. 3 Distribution of shear stress in the adhesive layer.**

Take the Laplace inverse of Eq. (16) to get

$$p_2(x,t) = p_0\left\{(1+c)\,\mathcal{L}^{-1}\left[\frac{\sinh(\alpha x)}{s\cdot\sinh(\alpha\ell)}\right]\right.$$

$$\left. + c\mathcal{L}^{-1}\left[\frac{\sinh[\alpha(\ell-x)]}{s\cdot\sinh(\alpha\ell)}\right] - cH(t)\right\} \tag{17}$$

For the special case $a_1 = 0$, the solution can be obtained in terms of infinite series.[6] As discussed earlier, $a_1 = 0$ represents the adhesive behavior described by a three-parameter solid (insert in Fig. 1) and observed experimentally in Ref. 1. For this case, the solution of Eq. (14) is

$$p_2(x,t) = p_0\left((1+c)\left\{\frac{\sinh(\sqrt{c_1}x)}{\sinh(\sqrt{c_1}\ell)} + \sum_{n=1}^{\infty}(-1)^n \frac{2n\pi}{c_1\ell^2 + n^2\pi^2}\right.\right.$$

$$\times \sin\left(\frac{n\pi x}{\ell}\right)\exp\left[-\left(\frac{1}{b_1} + \frac{n^2\pi^2}{b_1 c_1 \ell^2}\right)t\right]\Bigg\}$$

$$+ c\left\{\frac{\sinh[\sqrt{c_1}(\ell-x)]}{\sinh(\sqrt{c_1}\ell)} - \sum_{n=1}^{\infty}\frac{2n\pi}{c_1\ell^2 + n^2\pi^2}\right.$$

$$\left.\left.\times \sin\left(\frac{n\pi x}{\ell}\right)\exp\left[-\left(\frac{1}{b_1} + \frac{n^2\pi^2}{b_1 c_1 \ell^2}\right)t\right]\right\}\right) \tag{18}$$

where

$$c_1 = \frac{2k_1}{h_3}\left[\frac{1-\nu_1^2}{E_{11}h_1} + \frac{1-\nu_{2x}\nu_{2z}}{E_{2x}h_2}\right]$$

## Example

As an example, consider a case when the materials joined together are isotropic with $E_{11} = E_{2x} = 71.0$ GPa ($10.3\times 10^6$ psi), $\nu_1 = \nu_{2x} = \nu_{2z} = 0.33$, $h_1 = h_2 = 6.3$ mm (0.25 in.), $h_3 = 0.15$ mm (0.006 in.), and lap length of 25.4 mm (1.0 in.). Adhesive behavior shown in Fig. 1 is used. For the adhesive behavior, $k_1 = 100$ MPa (14.56 ksi) and $b_1 = 2.508$. Distribution of force in adherend 2, $p_2(x,t)$, as a function of distance from the end of the joint (insert in Fig. 2) at various times is shown in Fig. 2. The distribution changes its shape with time, and after an elapse of about 2 h it becomes almost a straight line. The shear stress distribution is obtained from

$$\tau(x,t) = \frac{\partial p_2(x,t)}{\partial x} \tag{19}$$

The distribution of shear stress in the adhesive layer is shown in Fig. 3 for various values of time $t$. At the time of application of the load, the shear stress has very large values at the ends of the joint, and the shear stress in the central portion is zero. The peaks in shear stresses gradually reduce with time, and, after about 2 h, the shear stress distribution within the length of the joint is fairly uniform.

The variation of shear stress and therefore that of shear strain in the adhesive layer is a function of time for various values of $x$. The analysis indicates that the shear strain drops sharply with time at $x = 0$ and then gradually increases. The shear strain in the central portion of the joint increases with time and stabilizes after about 2 h of load application.

## Conclusions

The maximum shear stress in the adhesive layer of a step-lap joint are considerably reduced when the time dependent behavior is taken into consideration. The shear distribution becomes fairly uniform after about 2 h.

## Acknowledgment

This work was performed under Northrop's Independent Research and Development Program.

## References

[1] Romanko, J. and Knauss, W. G., "Fatigue Behavior of Adhesively Bonded Joints," AFWAL-TR-80-4037, Vols. I and II, April 1980.

[2] Erdogan, F. and Ratwani, M. M., "Stress Distribution in Bonded Joints," *Journal of Composite Materials*, Vol. 5, July 1971, pp. 378-393.

[3] Satyanarayen, M., "Crack in a Thin Infinite Plate of Viscoelastic Medium," *AIAA Journal*, Vol. 12, Feb. 1974, pp. 233-235.

[4] Hughes, E. J. and Rutherford, J. L., "Selection of Adhesives for Fuselage Bonding," The Singer Company, Kearfott Division, Little Falls, N. J., Final Rept. KD-75-37, July 1975.

[5] Ratwani, M. M., "Characterization of Fatigue Crack Growth in Bonded Structures," AFFDL-TR-77-31, Vols. I and II, July 1977.

[6] *Tables of Integral Transforms*, Vol. I, edited by A. Erdelyi, McGraw-Hill Book Co., New York, N.Y., 1954.